AGU PUBLICATIONS

JGR

Journal of Geophysical Research: Space Physics

RESEARCH ARTICLE

10.1002/2016JA023755

Key Points:

- The first hypervelocity dust impact detection by the Cluster spacecraft
- The concept of dust impact detection with electric field instruments is discussed
- The size and velocity of impinging dust grains are estimated

Correspondence to:
J. Vaverka,
jakub.vaverka@umu.se

Citation:
Vaverka, J., A. Pellinen-Wannberg, J. Kero, I. Mann, A. De Spiegeleer, M. Hamrin, C. Norberg, and T. Pitkänen (2017), Detection of meteoroid hypervelocity impacts on the Cluster spacecraft: First results, *J. Geophys. Res. Space Physics*, *122*, doi:10.1002/2016JA023755.

Received 16 DEC 2016
Accepted 8 JUN 2017
Accepted article online 14 JUN 2017

Detection of meteoroid hypervelocity impacts on the Cluster spacecraft: First results

Jakub Vaverka[1], **Asta Pellinen-Wannberg**[1,2], **Johan Kero**[2], **Ingrid Mann**[3], **Alexandre De Spiegeleer**[1], **Maria Hamrin**[1], **Carol Norberg**[1,2], **and Timo Pitkänen**[1]

[1]Department of Physics, Umeå University, Umeå, Sweden, [2]Swedish Institute of Space Physics, Kiruna, Sweden, [3]Arctic University of Norway, Tromsø, Norway

Abstract We present the first study of dust impact events on one of the Earth-orbiting Cluster satellites. The events were identified in the measurements of the wide band data (WBD) instrument on board the satellite operating in monopole configuration. Since 2009 the instrument is operating in this configuration due to the loss of three electric probes and is therefore measuring the potential between the only operating antenna and the spacecraft body. Our study shows that the WBD instrument on Cluster 1 is able to detect pulses generated by dust impacts and discusses four such events. The presence of instrumental effects, intensive natural waves, noncontinuous sampling modes, and the automatic gain control complicates this detection. Due to all these features, we conclude that the Cluster spacecraft are not ideal for dust impact studies. We show that the duration and amplitudes of the pulses recorded by Cluster are similar to pulses detected by STEREO, and the shape of the pulses can be described with the model of the recollection of impact cloud electrons by the positively charged spacecraft. We estimate that the detected impacts were generated by micron-sized grains with velocities in the order of tens of km/s.

1. Introduction

Small dust and meteoroid hypervelocity ($v > 1$ km/s) impacts can cause satellite anomalies resulting in the worst case in loss of a spacecraft [*Caswell et al.*, 1995; *Lai et al.*, 2002; *Murad and Williams*, 2003; *Goel and Close*, 2015]. Such impacts threaten both manned and unmanned space missions. The dust flux into the Earth's atmosphere also influences atmospheric processes [cf. e.g., *Plane et al.*, 2015]. It is therefore important to study and quantify the dust flux that enters the Earth's atmosphere. The cosmic dust particles are part of the solar system and can feasibly be observed in the near-Earth space or when they enter the Earth's atmosphere [cf. e.g., *Grün et al.*, 1985, 1992; *Meyer-Vernet*, 2001; *Mann et al.*, 2011, 2014]. More studies of dust occurrence are required since a 2 orders of magnitude uncertainty about the meteoroid flux has been stated with different observation methods [see e.g., *Ceplecha et al.*, 1998; *Mathews et al.*, 2001; *Mann et al.*, 2011; *Plane*, 2012; *Plane et al.*, 2015]. One complementary method could be to use electric field instruments detecting an impact cloud generated by hypervelocity dust impacts [*Meyer-Vernet*, 2001; *Close et al.*, 2010]. This method has been successfully used for detection of pulses generated by dust impacts on spacecraft during several interplanetary missions such as the Voyager spacecraft crossing the Saturn ring plane [*Aubier et al.*, 1983; *Gurnett et al.*, 1983] followed by other missions such as Deep Space 1 [*Tsurutani et al.*, 2004], Cassini [*Wang et al.*, 2006; *Kurth et al.*, 2006; *Ye et al.*, 2014], Wind [*Malaspina et al.*, 2014; *Wood et al.*, 2015], and STEREO [*Meyer-Vernet et al.*, 2009; *Zaslavsky et al.*, 2012; *Zaslavsky*, 2015; *Malaspina et al.*, 2015]. The sensitivity of these measurements strongly depends on the design and operation of the electric field instrument.

In this study we use data from one of the four Cluster spacecraft launched in 2000 to study the Earth's magnetosphere, in order to evaluate whether it is possible to use its electric field measurements for searching for dust impacts in the near-Earth environment. We present the first observations of pulses generated by dust impacts on the Cluster 1 spacecraft which were detected by the wide band data (WBD) instrument [*Gurnett et al.*, 1997]. We first describe the mechanism of dust impact detection with the electric field instruments. Then we describe the specific properties of the Cluster spacecraft and the WBD instrument and their influence on dust detection, focusing on risks of misinterpretation of pulses generated by instrumental effects or by natural waves that are commonly present in the Earth's magnetosphere. We present and discuss some detected impacts and compare the observed pulses with the theoretical shape based on the model of electron

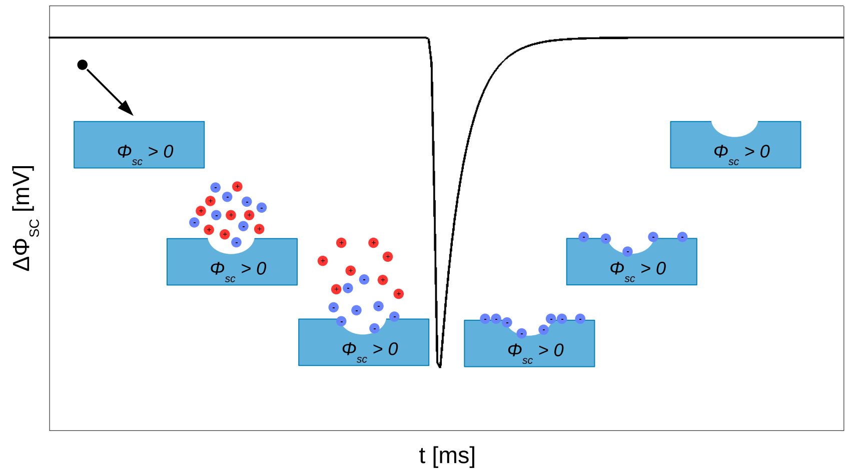

Figure 1. A simplifying sketch of the impact cloud (red ions and blue electrons) generation by a hypervelocity dust impact and the following electron recollection by a positively charged spacecraft body. The black line represents a dip in the temporal evolution of the spacecraft potential, Φ_{SC}, caused by the impact.

recollection described by *Zaslavsky* [2015]. We provide an estimate of the size and the velocity of the impinging grains and discuss the sensitivity of the method. In the last part we compare the first impact detected by the Cluster 1 spacecraft with impacts observed by the STEREO mission presented by *Zaslavsky* [2015].

2. Signals Generated by Dust Impacts

Dust impacts on spacecraft materials generate free electrons and ions by impact ionization, and this impact cloud alters the potential of the spacecraft or the antenna by recollecting the impact cloud particles if the spacecraft body is charged. The spacecraft potential, controlled by charging currents such as photoemission, collection of electrons and ions, and secondary electron emission, is an important parameter for the recollection of charged particles [*Garrett*, 1981, 2000]. The spacecraft is charged positively when illuminated by solar UV radiation, with photoemission as the dominant charging process. Electrons in the impact cloud are attracted to the positively charged spacecraft while the positive ions are repelled. The recollected electrons create an additional negative current to the spacecraft resulting in a fast reduction of the positive potential followed by a slower relaxation to the equilibrium value. This process is shown in a simplifying sketch in Figure 1. The recollection of particles is influenced by complex dynamic of the impact cloud and its expansion [*Pantellini et al.*, 2012]. The presence of positive ions close to the spacecraft surface influences the spacecraft potential when electrons are being recollected. Thus, the change in the spacecraft potential is influenced not only by recollection of electrons but also especially by dynamics of ions and their interaction with ambient electrons [*Meyer-Vernet et al.*, 2017]. Some electrons can be recollected by the antenna resulting in reduction of antenna potential. A slower relaxation time for the antenna potential could lead to a small "overshoot" in the measured electric field by a monopole antenna such as observed by STEREO [*Zaslavsky*, 2015], but this case is very unlikely for the Cluster spacecraft as detailed further below. The Active Spacecraft Potential Control feature, which can reduce the positive potential on Cluster 1 since August 2000, has not been operational [*Torkar et al.*, 2001].

There exist two different antenna operation modes of electric field instruments. Generally, the two modes have a small effect on electric field measurements but make a huge difference in dust impact detection capabilities. The instrument can either operate in a dipole regime, where the electric field is measured as a potential drop between two antennas, or in a monopole configuration where only one antenna is used with the spacecraft body as a reference. The monopole configuration is thus sensitive to changes in the spacecraft and antenna potentials, while the dipole configuration is sensitive only to changes in the antenna potentials [*Meyer-Vernet et al.*, 2014].

Each pulse generated by a dust impact can be described by three main parameters: the time constant for a first fast change of the potential, Δt, the amplitude of the pulse, $\Delta\Phi_{SC}$, and the time constant for the relaxation to the original value, τ. The time duration of the first fast voltage change is determined by the impact cloud dynamics.

The current reducing the spacecraft potential given by recollection of electrons and dynamics of cloud ions, I_{impact}, can be described by a Gaussian function, a simplified hypothesis suggested by *Zaslavsky* [2015],

$$I_{\text{impact}}(t) = \frac{Q_{\text{rec}}}{\sqrt{2\pi}\Delta t} e^{-(t-t_0)^2/2\Delta t^2}, \tag{1}$$

where Q_{rec} is the total amount of the recollected charge determining the amplitude of the pulse, Δt is the pulse rise time, and t_0 is time of the impact. The time needed to reach the equilibrium potential, Φ_{SC}, depends on the surrounding plasma environment [*Whipple*, 1981] and varies in the solar wind and in the different magnetospheric regions [*Vaverka et al.*, 2017]. The spacecraft potential decays exponentially back to the equilibrium state as the following [*Meyer-Vernet*, 1985]:

$$\Phi_{\text{SC}} \sim e^{-t/\tau}, \tag{2}$$

where τ is the relaxation time constant given by

$$\tau = \frac{CT_{\text{pho}}}{eSn_e} \sqrt{\frac{2\pi m_e}{eT_e}}, \tag{3}$$

where C is the spacecraft capacitance, S is the spacecraft surface area, T_{pho} is the photoelectron temperature, n_e is the plasma electron density, T_e is the ambient electron temperature, and m_e is the electron's mass. The pulse's shape can be estimated by convolution of (1) and (2) [*Zaslavsky*, 2015].

Analyzing the amplitude of a pulse in the spacecraft potential generated by the dust impact, $\Delta\Phi_{\text{SC}}$ gives a rough estimate of the size and the velocity of the impinging dust grain. The change of the spacecraft potential is given by the amount of charge recollected by the spacecraft, Q_{rec}, and by the spacecraft capacitance, C, as

$$\Delta\Phi_{\text{SC}} = Q_{\text{rec}}/C. \tag{4}$$

The Cluster spacecraft capacitance is close to 100 pF when using a spherical approximation. The number of recollected electrons depends on the amount of charge released by the dust impact, the energy of released electrons, and the spacecraft potential. The majority of the released electrons is attracted back to the spacecraft if the spacecraft potential is significantly higher than the energy of the released electrons. On the other hand, some electrons can escape when the spacecraft potential is on a similar level or lower. There are ion-electron collisions at the beginning of cloud expansion. Thus, the electrons are moving in random directions due to these collisions and can be recollected even when the positive spacecraft potential is low or even slightly negative [*Meyer-Vernet et al.*, 2017].

Laboratory experiments with hypervelocity dust impacts show that a typical electron temperature in the impact cloud is around 5 eV [*Collette et al.*, 2015, 2016]. This indicates that most of the electrons are recollected by a spacecraft at 1 AU distance from the Sun. The amount of the charge released by hypervelocity dust impacts has been experimentally studied [*Dietzel et al.*, 1973; *McBride and McDonnell*, 1999], resulting in a formula for an aluminium target [*McBride and McDonnell*, 1999]:

$$Q = 0.7m^{1.02}v^{3.48}, \tag{5}$$

where Q is the released charge, m is the mass of the impinging dust grain, and v is the velocity of the grain. Similar experiments have recently been revised for space relevant materials (germanium-coated black Kapton, beryllium copper, multilayer isolation, and solar cells) by *Collette et al.* [2014] resulting in a significantly lower yield. An equation for the released charge can be used in a general form:

$$Q = \alpha m^{\beta} v^{\gamma}, \tag{6}$$

where α, β, and γ are parameters depending on the target material. The parameter β is generally very close to 1, the value of γ is in the range of 3–5, and α is in the range of 10^{-1}–10^{-3} [*Collette et al.*, 2014]. Such a variation of parameters results in an uncertainty of the estimation of the released charge which depends on the target composition. It should be mentioned that these measurements have been performed for the impactor velocity between 10 and 40 km/s.

3. The Cluster Spacecraft and the Wide Band Data (WBD) Instrument

The Cluster mission comprises four identical spacecraft orbiting the Earth in close formation. The aim of this mission was to study the Earth's magnetosphere over the course of an entire solar cycle. The highly elliptical orbit with a perigee less than 4 Earth radii (R_E) and an apogee up to 20 R_E provides measurements from different parts of the Earth's magnetosphere and from the solar wind. The Cluster spacecraft are equipped with the Electric Fields and Waves (EFW) instrument [*Gustafsson et al.*, 2001]. Two pairs of dipole electric antennas each with boom length 44 m (88 m tip to tip) are placed on each spacecraft. There is a sphere of diameter 8 cm placed at the end of each of the antennas, and the electric field is measured as a potential drop between the two spheres. Each antenna is also equipped with a puck-shaped unit (8 cm diameter) placed 1.5 m in front of the sphere. The puck contains a preamplifier and shields the sphere from photoelectrons emitted from the spacecraft body. The large distance of the spheres from the spacecraft body and the shielding by the puck unit makes the recollection of impact cloud electrons by the antenna very unlikely. This is the reason why the dipole antennas on Cluster are less sensitive for dust impacts than the dipole detectors used, for example, during the Voyager, Cassini, Deep Space 1, and Wind missions. In practice only direct dust impacts on one of the spheres can be detected. Since the surface of the sphere is much smaller than the surface of the spacecraft, this path of dust detection is less probable.

There have occurred several probe failures on the satellites and only the Cluster 4 spacecraft still has four fully operational electric field probes. On the other hand, Cluster 1 has lost three probes and operates with only one electric antenna since November 2009. Since that time the electric field is measured as a potential drop between the only operating antenna and the spacecraft body. The shorter probe separation length (44 m instead 88 m) leads to an increased noise level in the electric field signals. Fortunately, this monopole configuration is sensitive to changes in the spacecraft potential and can thus be used for detecting hypervelocity dust impacts. We have used the data from the Cluster 1 spacecraft when it was operating in the monopole configuration to search for voltage pulses generated by dust impacts on the spacecraft body.

A signal from the electric field antenna is processed by the WBD instrument providing data with a high sampling frequency in three modes 27.4 kHz, 54.9 kHz, and 219.5 kHz [*Gurnett et al.*, 1997]. This corresponds to a time resolutions from 5 to 36 μs, which is high enough to detect signals generated by dust impacts, for which typical impact timescale is in order of a millisecond. The signal is digitized, with a 1 bit, 4 bit, or 8 bit resolution. Continuous sampling with full resolution (8 bit) is provided only in the slowest mode (27.4 kHz) because of limited data transmission. The 4 bit and 1 bit resolution could be provided to obtain continuous sampling in the faster modes. A noncontinuous sampling is typically used to maintain a full resolution. In this case 40 ms of data is followed by a 40 ms gap in the 54.9 kHz sampling mode, and 20 ms of data is followed by a 60 ms gap in the fastest mode. This reduces the total data coverage during the measurement to 50% in the 54.9 kHz mode and to 12.5% in the 219.5 kHz mode and complicates the dust impact detection.

Another feature of the WDB instrument is the automatic gain control providing sensitivity in a large dynamic range (75 dB) when the 8 bit resolution is used. The gain control has 16 levels with 5 dB steps which are used to provide a saturation level from 0.014 mV/m (gain 75) to 78 mV/m (gain 0). This property can strongly influence the dust grain detection by reaching the saturation threshold at high gain levels or by reducing the sensitivity at low gain levels. The influence of these effects for the dust impact detection is discussed in the following sections.

The WBD data are obtained only during a fraction of an orbit (∼4%) due to the lack of receiving ground stations. The limited amount of data, modes using noncontinuous sampling, and automatic gain control influencing dust impact detection must be considered carefully for the statistical analysis.

4. Observations

The measured data from the WBD instrument are complex since they contain large amounts of natural waves. Examples of such waves are electrostatic solitary waves [*Pickett et al.*, 2009, 2015] including monopolar, bipolar, and tripolar pulses and amplitude modulated electrostatic waves [*Deng et al.*, 2006] with fast oscillations in the electric field signal. Especially the bipolar and the monopolar pulses can be misinterpreted as dust impacts. The presence of solitary waves complicates identification of dust impacts. A better understanding of solitary waves and dust identification is needed for a complete statistical analysis. Also instrumental effects, such as the influence of the automatic gain control, interference with the Waves of High frequency and Sounder for

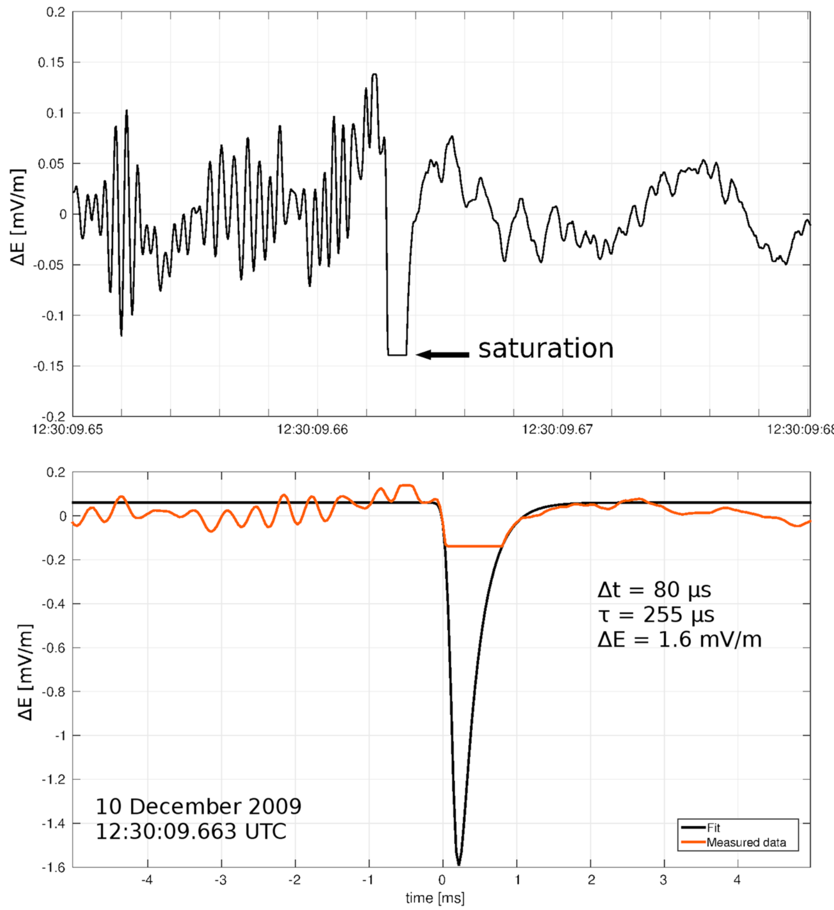

Figure 2. (top) A dust impact detected by the Cluster 1 spacecraft in the monopole configuration on 10 December 2009 at 12:30:09.6628 UTC when the WBD instrument operated in the continuous sampling mode with a sampling frequency of 27.4 kHz. A fast electric field drop is followed by a saturation at −0.14 mV/m (gain level 55 dB) for 692 μs and subsequently by a slower relaxation to the equilibrium value. (bottom) A fit of the theoretical pulse to the measured data. The best fit parameters are Δt = 80 μs as parameter of the Gaussian function, τ = 255 μs as a constant for the exponential decay ($e^{-t/\tau}$), and an amplitude of the pulse ΔE = 1.6 mV/m.

Probing of Electron density by Relaxation (WHISPER) instrument [*Décréau et al.*, 1997], and the presence of pulses generated by the switching between recordings of the electric and the magnetic field, can confuse the interpretation of the pulses. The automatic gain control generates pulses in connection to the change of the gain level. These pulses can easily be misinterpreted as dust impacts. Thus, we have removed data close to all gain changes (few milliseconds). Intensive pulses are generated when active sounding of the WHISPER experiment takes place. Data from these periods have also been excluded. We have developed a code for automatic searching for pulses in the measured electric field to find candidates for dust impacts. Fast changes in the electric field were used as a selection criteria. The events that have been identified using the automatic search method have been checked manually to distinguish them from the intensive natural wave background.

We have found four pulses that we interpret as dust impacts during this initial study. All impacts were detected while the WBD instrument was operational during crossing of the Earth's magnetopause in December 2009. An example of one of these impacts is shown in Figure 2 (top). This event occurred on 10 December 2009 at 12:30:09.6628 UTC when the WBD instrument was running in the continuous sampling mode with the sampling frequency of 27.4 kHz. It is possible to see that a fast electric field drop is followed by a saturation at −0.14 mV/m (gain level 55 dB) for 692 μs and after that by a slower relaxation back to the equilibrium value. The amplitude of the pulse is significantly larger than the ones of the surrounding natural waves. It is possible to see that natural waves are much weaker after the dust impact. The reason can be that the expanding impact cloud influences the local plasma and wave environment.

Table 1. The Range of the Pulse Parameters for the Dust Impacts by Cluster Compared With the Parameters Obtained by STEREO [*Zaslavsky*, 2015]

Parameter	Cluster	STEREO	STEREO Average Value
Δt (μs)	60–80	5–60	30
$\Delta\Phi_{SC}$ (mV)	6–70	15–150	
τ (μs)	100–500	100–1000	250

The Gaussian function and the consequential exponential relaxation to the original value, based on assumptions of recollection of electrons described by *Zaslavsky* [2015], are fitted to the observed pulse in Figure 2 (bottom). The best fit parameters are Δt = 80 μs as parameter of the Gaussian function (equation (1)), ΔE = 1.6 mV/m ($\Delta\Phi_{SC}$ = 70 mV) as the amplitude of the pulse (equation (4)), and τ = 255 μs as the constant for the exponential decay (equation (2)). The uncertainties of the fitted parameters is large because the main part of the pulse is in saturation and there are only few data points at the rising edge of the pulse. We estimate the relative uncertainties for τ to 30% and for Δt and $\Delta\Phi_{SC}$ at least to 50% (from the variation of fitting parameters). The precision of this fit is also influenced by the presence of a nonlinear response when the signal is close to the saturation level. The constant τ derived from equation (3) for T_e = 8 eV is in the range between 100 and 2000 μs because of uncertainty in the plasma electron density (n_e = 0.1–2 cm^{-3}), since there is no such data available from Cluster 1 during the dust impact. It is possible to see that the theoretical model fits to the measured data very well, and therefore, the detected pulse can be associated to the dust impact. This figure clearly shows the saturation effect caused by the automatic gain control: the expected peak amplitude in the fit to the shape of the pulse is in the measured data cutoff at −0.14 mV/m (gain level = 55 dB). The values of these parameters for the four detected dust impacts are in ranges Δt = 60–80 μs, τ = 100–500 μs, and ΔE = 0.14–1.6 mV/m ($\Delta\Phi_{SC}$ = 6–70 mV). These values correspond to the recollected charge Q = 0.6–7 pC. The parameters are listed in Table 1. The corresponding pulses are shown in Figure 3 with fitted peaks.

4.1. Estimation of the Size and the Velocity of Impacting Grains

We use four different sets of material parameters to show their influence on the quantitative analysis of the dust impacts detected by the Cluster spacecraft. We compare the commonly used relation for the amount of charge released by hypervelocity dust impacts given in equation (5) for an aluminium target (α = 0.7, β=1.02, and γ = 3.48) with three space related materials, beryllium copper (BeCu: $\alpha = 1.2 \cdot 10^{-2}$, β=1, and γ = 3.8), multilayer thermal isolation (MLI: $\alpha = 1.7 \cdot 10^{-3}$, β=1, and γ = 4.7), and solar cell surface ($\alpha = 4.7 \cdot 10^{-3}$, β=1, and γ = 4.2) [*Collette et al.*, 2014]. Figure 4 (top) shows the relation between the size and the velocity of the impinging dust grain shown in Figure 2 (ΔE = 1.6 mV/m) for the different target compositions. The grain is assumed to be spherical with a specific density of 2000 kg/m^3 typical for dust grains in space. The strong variation in target material parameters (α and γ) results only in a small variation of the derived impact parameters. Since the typical impact velocity derived from meteor observations is between 20 and 60 km/s [*Szasz et al.*, 2008] the observed pulse can be generated by a micron-sized grain in this velocity range. Similar values are observed with dust instruments in the interplanetary medium. For instance, for Ulysses the impact speeds that are derived from the signals range from 2 km/s to 70 km/s, while a significant fraction of registered events is caused by impacts of fast and small dust particles outside of the range of instrument calibration [*Mann*, 2010]. The hatched areas in Figure 4 show the typical impact velocity range for solar system dust particles. In some cases the relative impact velocity can be very low, for example, for the interstellar dust due to the Earth's orbital velocity. The observed pulse can be generated by a grain of radius $r \sim 10$ μm for an impact velocity lower than 10 km/s. Based on the finding that nanometer-sized dust can be accelerated up to an order of solar wind speed at 1 AU [*Mann et al.*, 2007; *Czechowski and Mann*, 2010], we here concluded that a 300 km/s impact could also have generated the observed pulse.

The amplitudes of all the four impacts detected by the Cluster spacecraft are in the range of 0.14–1.6 mV/m. This results only in small variation of the estimated velocity and the size of the impinging grains. Figure 4 (bottom) shows the relation between the impact velocity and the dust size for the different scales of amplitude of the pulses generated by the dust impact. We use the solar cell material since solar cells cover most of the Cluster spacecraft body. The lines correspond to the dynamical range of the WBD instrument (gain 0 dB–78 mV/m and gain 75 dB–0.014 mV/m) showing its sensitivity. It is possible to see that the WBD instrument can detect a dust grain of radius r = 10 μm impinging at 1 km/s when it operates in high gain level (75 dB)

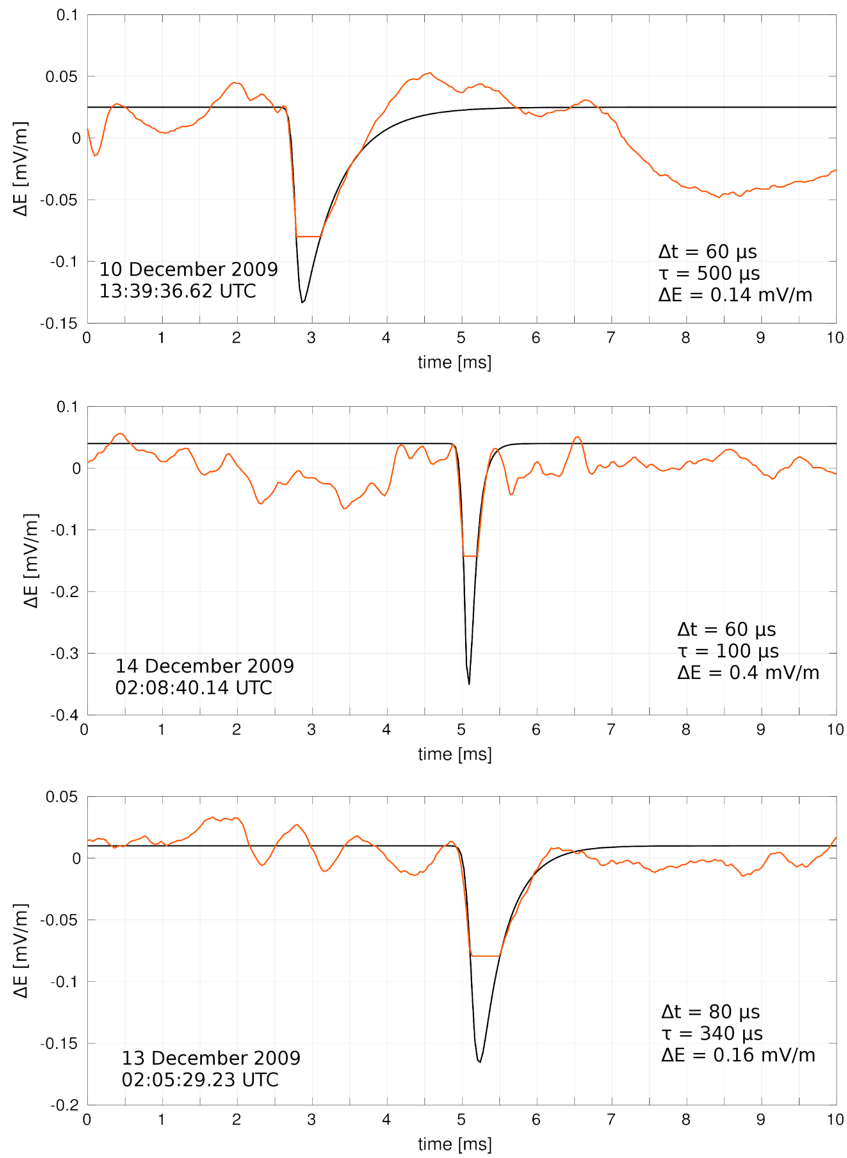

Figure 3. Fit of the theoretical pulse to the measured data for other registered dust impacts.

and at 10 km/s when it operates in the lowest gain level (0 dB). Grains of radius $r = 10$ nm can be detected only if they impact at velocity $\sim$ 300 km/s and the WBD instrument simultaneously operates at one of the highest gain levels.

5. Comparison to the STEREO Measurement

Hypervelocity dust impacts have been detected by many other missions mainly by electric field instruments in dipole configuration. STEREO spacecraft are equipped with an electric field instrument in monopole configuration [*Bougeret et al.*, 2008]. Impacts detected by STEREO can thus be compared with the first impacts detected by Cluster. The STEREO mission consists of two identical spacecraft orbiting the Sun approximately at 1 AU, measuring in the solar wind. STEREO has a much shorter electric field antenna (6 m length) which makes collection of electrons by the antenna possible. This is the main difference between STEREO and Cluster measurements, and the reason why the curve observed with Cluster has no overshoots. In the present study we use the same model for description of the pulse shape as used by *Zaslavsky* [2015] for the STEREO measurements. The main part of the curve shown in Figure 1 is determined by recollection of electrons and dynamics of ions and their interaction with ambient electrons. The time duration of pulses is about the same for both missions. The time constant τ is in the range from 100 μs to 1 ms for STEREO with a maximum at

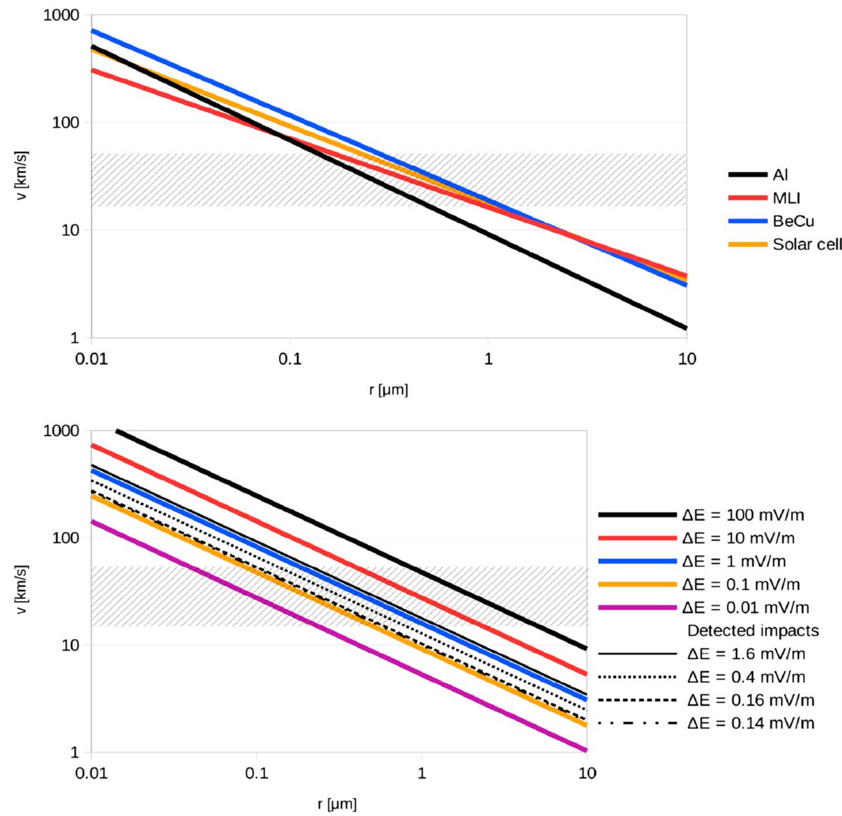

Figure 4. (top) The relation between the velocity and the size of the impinging grain shown in Figure 2 for different target materials: aluminium (Al), multilayer isolation (MLI), beryllium cooper (BeCu), and solar cell. (bottom) The same relation for different possible amplitudes of pulses, ΔE. The four thin black solid and dashed lines represent pulses detected by the Cluster spacecraft. The hatched areas show the typical impact velocity range for solar system dust particles.

250 μs [*Zaslavsky*, 2015] and in the range from 100 μs to 500 μs for Cluster. The constant of the Gaussian function, Δt, is close to 30 μs for STEREO while it is in the range from 60 to 80 μs for Cluster. This difference can be due to different construction of the spacecraft or by their different plasma environments. STEREO operates only in the solar wind, while Cluster detected the dust impacts during crossing of the Earth's magnetopause. In order to understand the difference in the constant of the Gaussian function, more impacts on Cluster must be analyzed.

The amplitude of the impacts detected by STEREO is influenced by the saturation level of the STEREO/WAVES time domain sampler (TDS) instrument because only pulses smaller than the 150 mV have been recorded in order to avoid signal distortion near saturation. The saturation level is 175 mV (30 mV/m, 6 m antenna), and the pulses of the amplitude from a few millivolts up to 150 mV (the detection level) have been recorded. Pulses observed by Cluster are in saturation, and their full amplitude is estimated by fitting of theoretical profile. Estimated amplitudes are from 0.14 mV/m (6.2 mV) to 1.6 mV/m (70 mV) and correspond to similar numbers as observed by the STEREO spacecraft. This gives a hint that these pulses can be generated by grains of a similar size-velocity ratio. The fact that pulses observed by the Cluster and the STEREO spacecraft have similar shape, duration, and amplitude proposes that these pulses might be generated by the same mechanism of recollection of electrons from the impact cloud generated by the hypervelocity dust impact. The range of the pulse parameters for the four detected dust impacts by Cluster and the parameters obtained from thousands of impacts by STEREO [*Zaslavsky*, 2015] is listed in Table 1.

6. Discussion and Conclusion

We have successfully detected the first hypervelocity impacts of dust on the Cluster 1 spacecraft with the WBD instrument. All four impacts were detected during crossing of the Earth's magnetopause in December 2009. The fact that the electric field instrument is forced to operate in a monopole configuration after several antenna failures made this detection possible. We have shown that this instrument is able to detect pulses generated by dust impacts in the monopole configuration.

The detection of pulses in the electric field data generated by the dust impacts on the Cluster spacecraft is difficult and perturbed by the presence of instrumental effects, intensive natural waves, noncontinuous sampling modes, and the automatic gain control adjusting the dynamic range between 0.014 mV/m and 78 mV/m. The presence of intense natural waves makes the automatic detection of dust impacts more challenging, and some of the waves can also be misinterpreted as pulses generated by dust impacts. Due to all these features, we conclude that the Cluster spacecraft are not ideal for dust impact studies. All these effects are necessary to keep in mind during the data processing and when comparing to data from other spacecraft since every instrument is unique with specific instrumental effects, duty cycle, and sensitivity.

We have shown that the shape of the pulses detected by Cluster corresponds to the model of the recollection of impact cloud electrons by a positively charged spacecraft described by *Zaslavsky* [2015] for the STEREO mission. The duration and the amplitudes of the first pulses recorded by Cluster are similar to pulses detected by STEREO using the monopole electric antenna which suggests that the pulses might have the same origin in dust impacts.

It is possible to estimate the size and the velocity of impinging dust grains from the amplitude of the measured pulse by applying an equation for the amount of the released free charge by hypervelocity impacts [*Collette et al.*, 2014]. The precision of this estimate is strongly influenced by the target composition, the spacecraft potential, the temperature of the impact cloud electrons, and by estimation of the peak amplitude in the case when the saturation is caused by the automatic gain control. On the other hand, very strong dependence of the amplitude of the pulse on the size (third power) and the velocity (third to fifth power) of the impacting grains allows this rough estimation. While it is not possible to distinguish between the slow heavy grain and the fast smaller one, we estimate possible combination of these parameters for the first impacts detected on the Cluster 1 spacecraft. The detected pulses can be generated by the impact of a micron-size grain with the velocity of the order of tens km/s or by a nanometer-size grain with the velocity of the order of hundreds km/s. However, small amount of detected pulses suggests that these impacts are probably generated by micron-size grains.

Applying charge production estimates to experimental results by *Collette et al.* [2014] we derive that the WBD instrument is able to detect dust grains of radii $r \sim 10$ μm impinging at 1 km/s when it operates in the high gain level (75 dB) and at 10 km/s when it operates in the lowest gain level (0 dB). Grains of radii $r \sim 10$ nm can be detected only when they impact at maximal expected velocity (~ 300 km/s) and the WBD instrument operates at one of the highest gain levels. Assuming that the typical impact velocity derived from meteor observations is close to 40 km/s [*Szasz et al.*, 2008], the lowest size limit for detection is 0.1 μm for the high gain level (75 dB) and 1 μm for the low gain level (0 dB).

We plan for a more detailed comparative study of signatures from dust impacts and solitary waves to reduce the risk of misinterpretation of these two features. After that a statistical study on impacts on Cluster spacecraft can be performed.

Acknowledgments
This work was supported by the Swedish National Space Board project dnr 110/14. We acknowledge the Cluster instrument teams and the Cluster Science Archive for providing publicly accessible data [*Laakso et al.*, 2010]. Johan Kero is supported by Swedish Research Council project grant 2012-4074.

References

Aubier, M. G., N. Meyer Vernet, and B. M. Pedersen (1983), Shot noise from grain and particle impacts in Saturn's ring plane, *Geophys. Res. Lett.*, *10*(1), 5–8.

Bougeret, J. L., et al. (2008), S/WAVES: The radio and plasma wave investigation on the STEREO mission, *Space Sci. Rev.*, *136*(1–4), 487–528.

Caswell, D. R., N. McBride, and A. Taylor (1995), Olympus end of life anomaly—A perseid meteoroid impact event?, *Int. J. Impact Engr.*, *17*(1–3), 139–150.

Ceplecha, Z., J. Borovička, W. G. Elford, D. O. Revelle, R. L. Hawkes, V. Porubčan, and M. Šimek (1998), Meteor phenomena and bodies, *Space Sci. Rev.*, *84*(3–4), 327–471.

Collette, A., E. Grün, D. Malaspina, and Z. Sternovsky (2014), Micrometeoroid impact charge yield for common spacecraft materials, *J. Geophys. Res. Space Physics*, *119*, 6019–6026.

Collette, A., G. Meyer, D. Malaspina, and Z. Sternovsky (2015), Laboratory investigation of antenna signals from dust impacts on spacecraft, *J. Geophys. Res. Space Physics*, *120*, 5298–5305, doi:10.1002/2015JA021198.

Collette, A., D. Malaspina, and Z. Sternovsky (2016), Characteristic temperatures of hypervelocity dust impact plasmas, *J. Geophys. Res. Space Physics*, *121*, 8182–8187, doi:10.1002/2015JA022220.

Close, S., P. Colestock, L. Cox, M. Kelley, and N. Lee (2010), Electrical anomalies on spacecraft due to hypervelocity impacts, *J. Geophys. Res.*, *115*, A12328, doi:10.1029/2010JA015921.

Czechowski, A., and I. Mann (2010), Formation and acceleration of nano dust in the inner heliosphere, *Astrophys. J.*, *714*(1), 89–99.

Décréau, P. M. E., et al. (1997), Whisper, a resonance sounder and wave analyser: Performances and perspectives for the Cluster mission, *Space Sci. Rev.*, *79*, 157–193.

Deng, X. H., et al. (2006), Observations of electrostatic solitary waves associated with reconnection by Geotail and Cluster, *Adv. Space Res.*, *37*(7), 1373–1381.

Dietzel, H., G. Eichhorn, H. Fechtig, E. Grun, H.-J. Hoffmann, and J. Kissel (1973), The HEOS 2 and HELIOS micrometeoroid experiments, *J. Phys. E: Sci. Instrum.*, *6*(3), 209–2017.

Garrett, H. B. (1981), The charging of spacecraft surfaces, *Rev. Geophys.*, *19*(4), 577–616.

Garrett, H. B. (2000), Spacecraft charging, an update, *IEEE Trans. Plasma Sci.*, *28*(6), 2017–2028.

Goel, A., and S. Close (2015), Electrical anomalies on spacecraft due to hypervelocity impacts, in *Proceedings of the Aerospace Conference, IEEE*, pp. 1–7, IEEE, Big Sky, Mont.

Grün, E., H. A. Zook, H. Fechtig, and R. H. Giese (1985), Collisional balance of the meteoritic complex, *Icarus*, *62*(2), 244–272.

Grün, E., H. Fechtig, J. Kissel, D. Linkert, D. Maas, J. A. M. McDonnell, G. E. Morfill, G. Schwehm, H. A. Zook, and R. H. Giese (1992), The ULYSSES dust experiment, *Astron. Astrophys. Suppl. Ser.*, *92*(2), 411–423.

Gurnett, D. A., E. Grün, D. Gallagher, W. S. Kurth, and F. L. Scarf (1983), Micron-sized particles detected near Saturn by the Voyager plasma wave instrument, *Icarus*, *53*(2), 236–254.

Gurnett, D. A., R. L. Huff, and D. L. Kirchner (1997), The wide-band plasma wave investigation, *Space Sci. Rev.*, *79*(1–2), 195–208.

Gustafsson, G., et al. (2001), First results of electric field and density observations by Cluster EFW based on initial months of operation, *Ann. Geophys.*, *19*(10), 1219–1240.

Kurth, W. S., T. F. Averkamp, D. A. Gurnett, and Z. Wang (2006), Cassini RPWS observations of dust in Saturn's E Ring, *Planet. Space Sci.*, *54*(9–10), 988–998.

Laakso, H., C. Perry, S. McCaffrey, D. Herment, A. J. Allen, C. C. Harvey, C. P. Escoubet, C. Gruenberger, M. G. G. T. Taylor, and R. Turner (2010), Cluster Active Archive: Overview, in *The Cluster Active Archive, Astrophysics and Space Science Proceedings*, pp. 3–37, Springer, Dordrecht, Netherlands.

Lai, S. T., E. Murad, and W. J. McNeil (2002), Hazards of hypervelocity impacts on spacecraft, *J. Spacecraft Rockets*, *39*(1), 106–114.

Malaspina, D. M., M. Horanyi, A. Zaslavsky, K. Goetz, L. B. Wilson, and K. Kersten (2014), Interplanetary and interstellar dust observed by the Wind/WAVES electric field instrument, *Geophys. Res. Lett.*, *41*, 266–272, doi:10.1002/2013GL058786.

Malaspina, D. M., L. E. O'Brien, F. Thayer, Z. Sternovsky, and A. Collette (2015), Revisiting STEREO interplanetary and interstellar dust flux and mass estimates, *J. Geophys. Res. Space Physics*, *120*(8), 6085–6100.

Mann, I. (2010), Interstellar dust in the solar system, *Annu. Rev. Astron. Astrophys.*, *48*, 173–203.

Mann, I., E. Murad, and A. Czechowski (2007), Nanoparticles in the inner solar system, *Planet. Space Sci.*, *55*(9), 1000–1009.

Mann, I., et al. (2011), Dusty plasma effects in near earth space and interplanetary medium, *Space Sci. Rev.*, *161*(1–4), 1–47.

Mann, I., N. Meyer-Vernet, and A. Czechowski (2014), Dust in the planetary system: Dust interactions in space plasmas of the solar system, *Phys. Rep.*, *536*(1), 1–39.

Mathews, J. D., D. Janches, D. D. Meisel, and Q. Zhou (2001), The micrometeoroid mass flux into the upper atmosphere: Arecibo results and a comparison with prior estimates, *Geophys. Res. Lett.*, *28*(10), 1929–1932.

Meyer-Vernet, N. (1985), Comet Giacobini-Zinner diagnosis from radio measurements, *Adv. Space Res.*, *5*(12), 37–46.

Meyer-Vernet, N. (2001), Detecting dust with electric sensors in planetary rings, comets and interplanetary space, in *Proceedings of the 7th International Conference, Spacecraft Charging Technology, ESTEC*, edited by R. A. Harris, pp. 635–640, ESA SP-476, Noordwijk, Netherlands.

Meyer-Vernet, N., M. Maksimovic, A. Czechowski, I. Mann, I. Zouganelis, K. Goetz, M. L. Kaiser, O. C. St. Cyr, J. Bougeret, and S. D. Bale (2009), Dust detection by the wave instrument on STEREO: Nanoparticles picked up by the solar wind?, *Sol. Phys.*, *256*(1–2), 463–474.

Meyer-Vernet, N., M. Moncuquet, K. Issautier, and A. Lecacheux (2014), The importance of monopole antennas for dust observations: Why Wind/WAVES does not detect nanodust, *Geophys. Res. Lett.*, *41*, 2716–2720, doi:10.1002/2014GL059988.

Meyer-Vernet, N., M. Moncuquet, K. Issautier, and P. Schippers (2017), Frequency range of dust detection in space with radio and plasma wave receivers: Theory and application to interplanetary nanodust impacts on Cassini, *J. Geophys. Res. Space Physics*, *122*, 8–22, doi:10.1002/2016JA023081.

McBride, N., and J. A. M. McDonnell (1999), Meteoroid impacts on spacecraft: Sporadics, streams, and the 1999 Leonids, *Planet. Space Sci.*, *47*(8–9), 1005–1013.

Murad, E., and I. Williams (2003), *Meteors in the Earth's Atmosphere: Meteoroids and Cosmic Dust and their Interactions With the Earth's Upper Atmosphere*, Cambridge Univ. Press, New York.

Pantellini, F., S. Landi, A. Zaslavsky, and N. Meyer-Vernet (2012), On the unconstrained expansion of a spherical plasma cloud turning collisionless: Case of a cloud generated by a nanometre dust grain impact on an uncharged target in spaces, *Plasma Phys. Controlled Fusion*, *54*(4), 045005.

Pickett, J. S., et al. (2009), Electrostatic solitary waves in current layers: From Cluster observations during a super-substorm to beam experiments at the LAPD, *Nonlinear Processes Geophys.*, *16*(3), 431–442.

Pickett, J. S., W. S. Kurth, D. A. Gurnett, R. L. Huff, J. B. Faden, T. F. Averkamp, D. Píša, and G. H. Jones (2015), Electrostatic solitary waves observed at Saturn by Cassini inside 10 Rs and near Enceladus, *J. Geophys. Res. Space Physics*, *120*, 6569–6580, doi:10.1002/2015JA021305.

Plane, J. M. C. (2012), Cosmic dust in the Earth's atmosphere, *Chem. Soc. Rev.*, *41*(19), 6507–6518.

Plane, J. M. C., W. Feng, and E. C. M. Dawkins (2015), The mesosphere and metals: Chemistry and changes, *Chem. Rev.*, *115*(10), 4497–4541.

Szasz, C., J. Kero, D. D. Meisel, A. Pellinen-Wannberg, G. Wannberg, and A. Westman (2008), Orbit characteristics of the tristatic EISCAT UHF meteors, *Mon. Not. R. Astron. Soc.*, *388*(1), 15–25.

Torkar, K., et al. (2001), Active spacecraft potential control for Cluster—Implementation and first results, *Ann. Geophys.*, *19*(12), 1289–1302.

Tsurutani, B. T., D. R. Clay, L. D. Zhang, B. Dasgupta, D. Brinza, M. Henry, J. K. Arballo, S. Moses, and A. Mendis (2004), Plasma clouds associated with Comet P/Borrelly dust impacts, *Icarus*, *167*(1), 89–99.

Vaverka, J., A. Pellinen-Wannberg, J. Kero, I. Mann, A. De Spiegeleer, M. Hamrin, C. Norberg, and T. Pitkänen (2017), Potential of Earth Orbiting Spacecraft Influenced by Meteoroid Hypervelocity Impacts, *IEEE Trans. Plasma Sci.*, *45*(5), 1–8.

Wang, Z., D. A. Gurnett, T. F. Averkamp, A. M. Persoon, and W. S. Kurth (2006), Characteristics of dust particles detected near Saturn's ring plane with the Cassini Radio and Plasma Wave instrument, *Planet. Space Sci.*, *54*(9–10), 957–966.

Whipple, E. C. (1981), Potentials of surfaces in space, *Rep. Prog. Phys.*, *44*(11), 1197–1250.

Wood, S. R., D. M. Malaspina, L. Andersson, and M. Horanyi (2015), Hypervelocity dust impacts on the Wind spacecraft: Correlations between Ulysses and Wind interstellar dust detections, *J. Geophys. Res. Space Physics*, *120*(9), 7121–7129.

Ye, S.-Y., D. A. Gurnett, W. S. Kurth, T. F. Averkamp, M. Morooka, S. Sakai, and J.-E. Wahlund (2014), Electron density inside Enceladus plume inferred from plasma oscillations excited by dust impacts, *J. Geophys. Res. Space Physics*, *119*(5), 3373–3380.

Zaslavsky, A. (2015), Floating potential perturbations due to micrometeoroid impacts: Theory and application to S/WAVES data, *J. Geophys. Res. Space Physics*, *120*(2), 855–867.

Zaslavsky, A., et al. (2012), Interplanetary dust detection by radio antennas: Mass calibration and fluxes measured by STEREO/WAVES, *J. Geophys. Res.*, *117*, A05102, doi:10.1029/2011JA017480.